Title
Characterization of the Optical Modes in 3D-Periodic Arrays of Metallic Nanospheres

ISBN
9781424451173

Authors
Campione, Salvatore
Steshenko, Sergiy
Albani, Matteo
et al.

Publication Date
2011-08-01

DOI
10.1109/ursigass.2011.6050345

Characterization of the Optical Modes in 3D-Periodic Arrays of Metallic Nanospheres

Salvatore Campione[1], Sergiy Steshenko[2,3], Matteo Albani[2], and Filippo Capolino[1]

[1]Department of Electrical Engineering and Computer Science, University of California, Irvine, CA, 92697-2625, USA
scampion@uci.edu , f.capolino@uci.edu

[2]Department of Information Engineering, University of Siena, 53100, Siena, Italy
sergiy.steshenko@gmail.com , matteo.albani@ing.unisi.it

[3]Institute of Radiophysics and Electronics of the National Academy of Sciences of Ukraine, 61085, Kharkiv, Ukraine

Abstract

Complex optical modes in 3D-periodic arrays of metallic nanospheres are analyzed at optical frequencies for both longitudinal and transversal (with respect to the mode traveling direction) polarization states. Each nanosphere of the array is modeled to act as a single dipole by using the single dipole approximation approach, and the metal permittivity is described by the Drude model. Complex mode dispersion diagrams, the figure of merit and effective refractive index versus frequency are shown and compared with those obtained with Maxwell Garnett homogenization theory. Comparison with effective permittivity retrieved by scattering parameters of finite-thickness structures will be shown during the presentation.

1. Introduction

3D-periodic arrays of nanospheres can be engineered to obtain peculiar characteristics, such as, among others, slow wave structures, and double negative materials. We analyze here a 3D-periodic metamaterial made of a collection of plasmonic nanospheres, and in particular how waves propagate inside the metamaterial. Mode analysis of 3D-periodic arrays of dielectric and magneto-dielectric nanospheres have been analyzed in [1], whereas in the case of metallic nanospheres in [1-2]. In [2], the authors adopted the nanotransmission line network concept to design broadband negative refractive index materials, focusing only on the transversal polarization (with respect to the direction of propagation of the modes) that allows for backward propagation. Also, they considered densely packed and properly designed 3D-periodic arrays since they may support a nanotransmission line propagating mode and thus may act as an effective negative-index metamaterial. In this paper, we analyze the complex optical modes in 3D-periodic arrays of metallic nanospheres for both longitudinal and transversal (with respect to the mode traveling direction) polarization states. We present a structure that is able to boost the figure of merit (defined as the ratio between the real and the imaginary part of the effective refractive index) in such a periodic structure. The effective refractive index obtained by the modal analysis for transverse polarization is compared to the one from Maxwell Garnett homogenization theory.

2. Formulation

The structure analyzed in this paper is a 3D-periodic array of metallic nanospheres, as in Fig. 1. The monochromatic time harmonic convention, $\exp(-i\omega t)$, is assumed here and throughout the paper, and is therefore suppressed hereafter. Moreover, in the following equations, bold letters refer to vector quantities, a caret on top of a bold letter refers to unit vector quantities, and a bar under a bold letter refers to dyadic quantities.

Single dipole approximation (SDA) [3] is adopted to model each nanosphere to act as a single electric dipole in the case of small nanospheres (with respect to the wavelength) close to their fundamental resonance frequency. According to SDA, the induced dipole moment is $\mathbf{p} = \alpha_{ee}\mathbf{E}^{loc}$, with α_{ee} being the electric polarizability of the nanosphere (expressions for α_{ee} can be found in [3]; here, we adopt the one according to Mie theory), and $\mathbf{E}^{loc}$ is the local field produced by all the nanospheres of the array except the considered nanosphere plus the external incident field to the array. Considering the nanosphere in position $\mathbf{r}_0 = x_0\hat{\mathbf{x}} + y_0\hat{\mathbf{y}} + z_0\hat{\mathbf{z}}$, it follows that

978-1-4244-6051-9/11/$26.00 ©2011 IEEE

$\mathbf{E}^{\text{loc}}(\mathbf{r}_0,\mathbf{k}_\text{B}) = \mathbf{E}^{\text{inc}}(\mathbf{r}_0) + \underline{\breve{\mathbf{G}}}^{\infty}(\mathbf{r}_0,\mathbf{r}_0,\mathbf{k}_\text{B})\cdot\mathbf{p}_0$, where $\mathbf{k}_\text{B} = k_x\hat{\mathbf{x}} + k_y\hat{\mathbf{y}} + k_z\hat{\mathbf{z}}$ is the wavevector of the plane wave or quasi-periodic excitation, for which each nanosphere will have an electric dipole moment equal to $\mathbf{p}_n = \mathbf{p}_0 e^{i\mathbf{k}_\text{B}\cdot\mathbf{d}_n}$, $\mathbf{d}_n = n_1 a\hat{\mathbf{x}} + n_2 b\hat{\mathbf{y}} + n_3 c\hat{\mathbf{z}}$, with $n_1, n_2, n_3 = 0,\pm1,\pm2,\ldots$, $\mathbf{E}^{\text{inc}}(\mathbf{r}_0)$ is the incident field and $\underline{\breve{\mathbf{G}}}^{\infty}(\mathbf{r}_0,\mathbf{r}_0,\mathbf{k}_\text{B})\cdot\mathbf{p}_0$ is the field produced by all the nanospheres but the one in position $\mathbf{r}_0$, with $\underline{\breve{\mathbf{G}}}^{\infty}(\mathbf{r}_0,\mathbf{r}_0,\mathbf{k}_\text{B})$ being the regularized dyadic Green's function. Substituting then the expression for the local field into the aforementioned induced dipole moment equation, we get $\mathbf{p}_0 = \alpha_{\text{ee}}\left[\mathbf{E}^{\text{inc}}(\mathbf{r}_0) + \underline{\breve{\mathbf{G}}}^{\infty}(\mathbf{r}_0,\mathbf{r}_0,\mathbf{k}_\text{B})\cdot\mathbf{p}_0\right]$ which, in absence of excitation, leads to the homogeneous linear system $\underline{\mathbf{A}}(\mathbf{k}_\text{B}) \triangleq \underline{\mathbf{I}} - \alpha_{\text{ee}}\underline{\breve{\mathbf{G}}}^{\infty}(\mathbf{r}_0,\mathbf{r}_0,\mathbf{k}_\text{B}) = 0$ with $\underline{\mathbf{I}}$ being the unit dyad. Complex mode analysis in the 3D-periodic array is then performed by computing the complex zeroes of the determinant of $\underline{\mathbf{A}}(\mathbf{k}_\text{B})$. The computation of $\underline{\breve{\mathbf{G}}}^{\infty}(\mathbf{r}_0,\mathbf{r}_0,\mathbf{k}_\text{B})$ involves slowly convergent series, which diverge for complex values of the wavenumber $\mathbf{k}_\text{B}$. The solution adopted in this work makes use of Ewald's method, which provides series with Gaussian convergence and only a handful of terms are needed [4]. The dyadic form of the Ewald representation of the periodic Green's function evaluation used in this paper will be provided in [5].

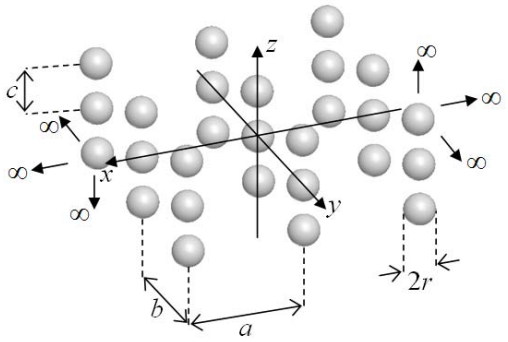

Fig. 1. 3D-periodic array of metallic nanospheres under analysis embedded in a homogeneous medium with permittivity ε_h. The radius of each nanosphere is *r*; *a*, *b* and *c* are the periodicities along *x*-, *y*- and *z*-direction, respectively.

We analyze the optical complex modes traveling along the *z*-direction in a 3D-periodic array of silver nanospheres in free space (with background wavenumber k_0), for both transversal and longitudinal polarization states with respect to the mode traveling direction (T- and L-pol, respectively), accounting also for metal losses. In the L-pol case, each nanosphere has an induced dipole moment along the *z*-direction (i.e., $\mathbf{p} = p_z\hat{\mathbf{z}}$). In the T-pol case, each nanosphere has an induced dipole moment orthogonal to *z*. The adopted Drude model parameters for silver are $\varepsilon_\infty = 5$, plasma frequency $\omega_p = 1.37\times10^{16}$ rad/s and damping factor $\gamma = 27.3\times10^{12}\,\text{s}^{-1}$ [6]. The radius of each nanosphere is $r = 25$ nm. We analyze two structures with A) $a = b = c = 75$ nm and B) $a = b = 150$ nm, $c = 75$ nm.

3. Dispersion Diagrams

The dispersion diagram for T-pol for structure B is reported in Fig. 2. This structure exhibits low imaginary part of the modal wavenumbers with respect to structure A. Looking at the positive *z*-direction, the physical modes are those modes with $\alpha_z \geq 0$ (see [5] for details). Then, a backward mode is defined for $\beta_z\alpha_z < 0$, whereas a forward one is defined for $\beta_z\alpha_z > 0$. The evolution of the same modes in the complex k_z plane is shown in Fig. 2(c). The dispersion diagram for L-pol is shown in Fig. 3. Note that the T-pol can propagate over a large range of frequencies, especially at low frequency, whereas the L-pol can propagate with small losses only over a very narrow frequency range.

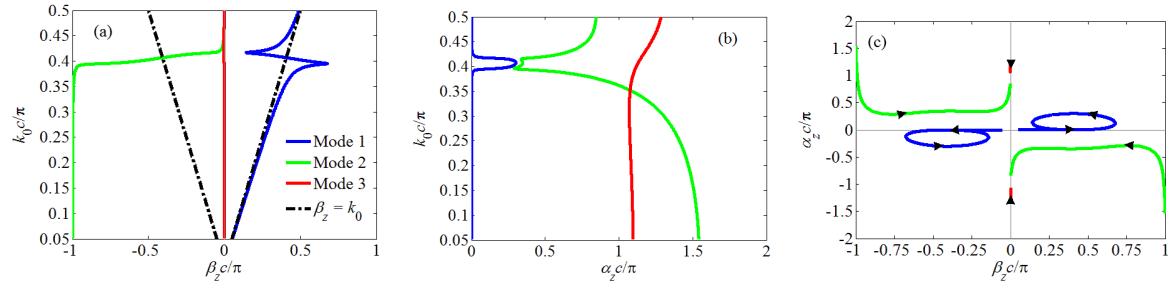

Fig. 2. Dispersion diagram for T-pol for structure B. (a) Real part and (b) imaginary part of the wavenumber $k_z = \beta_z + i\alpha_z$, only for the physical modes having $\alpha_z \geq 0$. Also, 'Mode 3' has a negative real part, very close to zero. (c) Modes in the complex k_z plane for T-pol for structure B. Arrows indicate direction of increasing frequency.

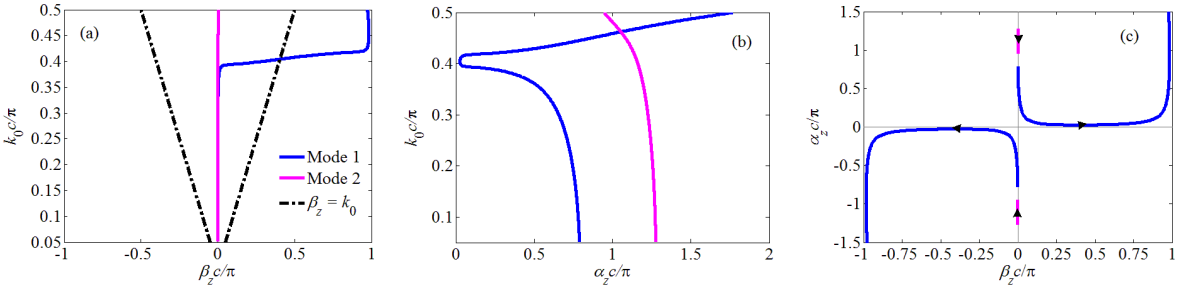

Fig. 3. As in Fig. 2, for L-pol. Also, 'Mode 2' has a positive real part, very close to zero. In a small frequency region, low loss propagation is allowed.

4. Effective Refractive Index

The effective refractive index of structure A is computed for the T-pol by normalizing the wavenumber found as in the previous section and by also using the Maxwell Garnett formulas with two different polarization expressions, the one from Mie theory and the quasi static one (also called Clausius-Mossotti, CM). The three methods provide comparable results as shown in Fig. 5. Note that large values of refractive index are obtained, as well as very low ones, showing that this material can provide an epsilon near zero (ENZ) artificial medium in a narrow frequency band. Losses can be rather low, in the low frequency region, as also shown by the figure of merit in Fig. 4.

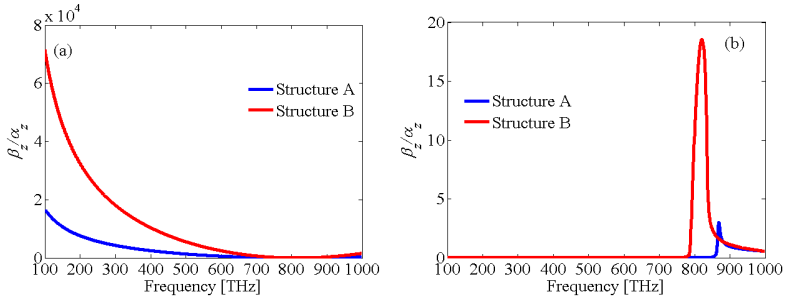

Fig. 4. Comparison between the figure of merit *F* of the 'Mode 1' in the two analyzed structures versus frequency. (a) Transversal and (b) longitudinal polarization.

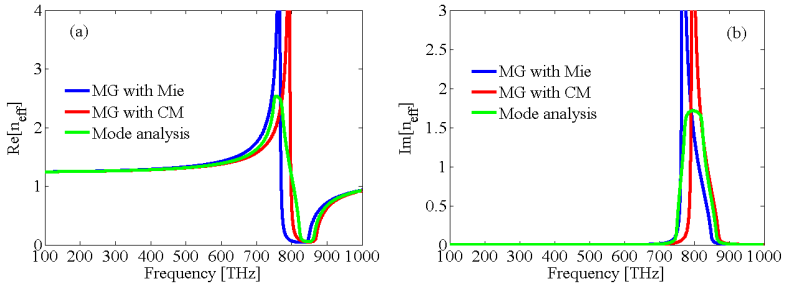

Fig. 5. Real and imaginary part of the refractive index of the 'Mode 1', T-pol, structure A, versus frequency. Three methods: (i) by normalizing the modal wavenumber, (ii) and (iii) by the Maxwell Garnett theory, with two different polarization expressions.

5. Conclusion

This work provided a description of complex modal analysis in 3D-periodic arrays of metallic nanospheres. Effective parameters obtained by Maxwell Garnett have been shown and compared with those obtained by a modal analysis. A further comparison with those retrieved by the scattering parameters will be shown in the presentation.

6. Acknowledgement

The authors acknowledge partial support from the European Commission 7th Framework Program FP7/2008, "NMP-2008-2.2-2 Nanostructured meta-materials", grant "Metachem" number 228762.

7. References

1. R.A. Shore, and A.D. Yaghjian, *Complex Waves on 1D, 2D, and 3D Periodic Arrays of Lossy and Lossless Magnetodielectric Spheres,* AFRL-RY-HS-TR-2010-0019 (Air Force Research Laboratory, 2010).

2. A. Alu, and N. Engheta, "Three-dimensional nanotransmission lines at optical frequencies: A recipe for broadband negative-refraction optical metamaterials," *Phys. Rev. B,* **75**, 024304, 2007.

3. S. Steshenko, and F. Capolino, "Single Dipole Approximation for Modeling Collection of Nanoscatterers," in *Theory and Phenomena of Metamaterials*, F. Capolino, ed., Boca Raton, FL, CRC Press, 2009, p. 8.1.

4. P. Myun-Joo, P. Jongkuk, and N. Sangwook, "Efficient calculation of the Green's function for the rectangular cavity," *IEEE Microwave and Guided Wave Letters*, **8**, 1998, pp. 124-126.

5. S. Campione, S. Steshenko, M. Albani, and F. Capolino, "Complex Modes in 3D-Periodic Arrays of Plasmonic Nanospheres", to be submitted, 2011.

6. I. El-Kady, M. M. Sigalas, R. Biswas, K. M. Ho, and C. M. Soukoulis, "Metallic photonic crystals at optical wavelengths," *Phys. Rev. B,* **62**, 15299, 2000.